Influence of illumination incidence angle, grain size and grain boundary recombination velocity on the facial solar cell diffusion capacitance

M.M. Deme, S. Mbodji, S. Ndoye, A. Thiam, A. Dieng and G. Sissoko

Laboratoire des Semi-Conducteurs et d'Energie Solaire,
Département de Physique, Faculté des Sciences et Techniques,
Université Cheikh Anta Diop, B.P. 5005, Dakar Fann, Sénégal

(reçu le 24 Février 2010 – accepté le 25 Mars 2010)

Abstract - *A theoretical 3D study on the diffusion capacitance in a polycrystalline silicon solar cell under steady multispectral light and various incidence angles is carried out. The effect of grain size, grain boundary recombination velocity and illumination incidence angle on the diffusion capacitance is then presented and analyzed; the dark capacitance of the cell was also calculated. Finally, considering the junction of the solar cell as plane capacitor, the efficiency is evaluated. The effect of grain size, grain boundary recombination velocity and illumination incidence angle have been discussed, based on the open circuit and short circuit capacitance modes.*

Résumé - *Une étude théorique à trois dimensions (3D) et en régime statique de la capacité de diffusion d'une cellule solaire au silicium polycristallin sous éclairement multispectral suivant un angle d'incidence variable est effectuée. L'influence de la taille de grain, de la vitesse de recombinaison aux joints de grain et de l'angle d'incidence de l'éclairement est présentée et analysée. La capacité de diffusion intrinsèque de la cellule est aussi déterminée. Tenant compte des propriétés de la jonction qui est supposée être un condensateur plan, le rendement de la cellule solaire est évalué en se basant sur la capacité de diffusion en circuit ouvert et en court-circuit.*

Keywords: Grain size - Grain boundary recombination velocity - Incidence angle - Diffusion capacitance - Efficiency.

1. INTRODUCTION

This study is aiming at a 3D modelling a facial solar cell capacitance under steady multispectral illumination for different incidence angles.

The basic theory presented the model and calculations of expressions of excess minority carriers density, photo voltage and diffusion capacitance of the solar cell.

After computing the dark capacitance, we analyze the effect of grain size (g) [1-4], grain boundaries recombination velocity (Sgb) [1-4] and the illumination incident angle (q) [5] on the efficiency of the solar cell.

2. MODEL AND THEORY

We use figure1 to present the facial solar layout, the components of cell and an isolated grain. In figure 2, conditions of the illumination and characteristics of the isolated grain are presented.

Equation of continuity for excess minority carriers density $\delta(x,y,z)$ in the cell base is as follows:

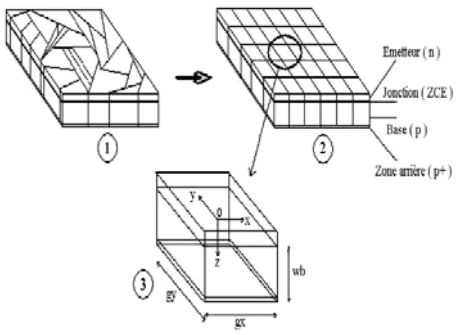

Fig. 1: Facial solar cell layout (1- cell grains; 2- components of a cell; 3- isolated grain)

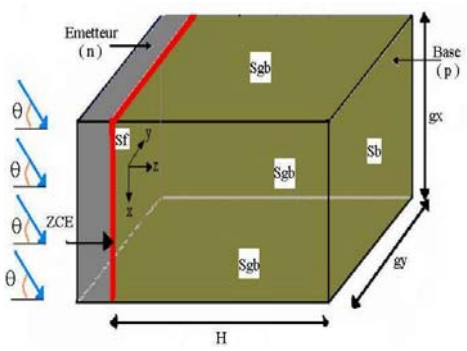

Fig. 2: Illumination incidence angles and grain boundaries recombination velocity symbols

$$D.\left[\frac{\partial^2\delta(x,y,z)}{\partial x^2}+\frac{\partial^2\delta(x,y,z)}{\partial y^2}+\frac{\partial^2\delta(x,y,z)}{\partial z^2}\right]-\frac{\delta(x,y,z)}{\tau}+G(x)=0 \quad (1)$$

D and τ represent respectively the diffusion coefficient of charge carriers and life duration of excess minority charge carriers generated in the base. $G(z)$ is the generation ratio measured at the base depth z for the charge carriers in case of steady state multispectral illumination base.

This quantity $G(z)$ is given as follows for various angular (θ) directions of incident light:

$$G(z) = (n.\cos\theta)\times\sum_{i=1}^{3} a_i \times \exp(-b_i.z) \quad (2)$$

Parameters a_i and b_i are in fact constant coefficients tabulated and defined through modelling linked to spectral absorption characterizing a solar cell under standard conditions AM = 1.5 and n = 1 sun, the parameter n being the number of suns.

Note that the mathematical solution for the above continuity equation is a super-sum of series [4]:

$$\delta(x,y,z) = \sum_k\sum_j Z_{kj}(z)\times\cos(c_k\times x)\times\cos(c_j\times y) \quad (3)$$

c_k and c_j being eigen values, they are derived through data linked to grain boundary conditions given below [4]:

$$D\times\left[\frac{\partial\delta(x,y,z)}{\partial x}\right]_{x=\pm\frac{gx}{2}} = \mp Sgb\times\delta\left(\pm\frac{gx}{2},y,z\right) \quad (4)$$

$$D\times\left[\frac{\partial\delta(x,y,z)}{\partial y}\right]_{y=\pm\frac{gy}{2}} = \mp Sgb\times\delta\left(x,\pm\frac{gy}{2},z\right) \quad (5)$$

Sgb represents the grain boundary recombination velocity while gx and gy are directional grain sizes.

Exploiting the cosinus orthogonality properties and inserting $\delta(x,y,z)$ into the equation n°1, below key relationships are derived as follows:

$$Z_{kj}(x) = A_{kj}.\cos h\left(\frac{z}{L_{kj}}\right) + B_{kj}.\sin h\left(\frac{z}{L_{kj}}\right) + \sum_{i=1}^{3} c_i.\exp(-b_i z) \qquad (6)$$

where

$$C_i = \frac{a_i L_{kj}^2.n.\cos(\theta)}{D_{kj}(1 - b_i^2 L_{kj}^2)} \qquad (7)$$

with

$$D_{kj} = \frac{D\left[C_k.gx + \sin(C_k.gx)\right].\left[C_k.gy + \sin(C_k.gy)\right]}{16.\sin\left(C_k.\frac{gx}{2}\right).\sin\left(C_j.\frac{gy}{2}\right)} \qquad (8)$$

And

$$L_{kj} = \sqrt{\frac{1}{\frac{1}{L^2} + C_k^2 + C_j^2}} \qquad (9)$$

While D_{kj} and L_{kj} are standing respectively for effective diffusion coefficient and effective diffusion length [4]. The coefficients A_{kj} and B_{kj} are constant quantities derived through boundary conditions analysis:

For the junction ($z = 0$)

$$D \times \left[\frac{\partial\delta(x,y,z)}{\partial z}\right]_{z=0} = Sf \times \delta(x,y,0) \qquad (10)$$

At the back edge of the base ($z = H$)

$$D \times \left[\frac{\partial\delta(x,y,z)}{\partial z}\right]_{z=H} = -Sb \times \delta(x,y,H) \qquad (11)$$

Sf is called junction recombination velocity and stands for a sum of two components:

Sf_0 [2, 6-8] and Sf_j . Sf_0 is an intrinsic recombination velocity while Sf_j is a parameter linked to the current flow in external load for a given operational point of the solar cell:

$$Sf = Sf_0 + Sf_j$$

Sb [9] is a recombination velocity occurring on the back surface of the cell. It quantifies the rate at which excess minority carriers are let at the rear side of the solar cell.

The diffusion capacitance [10] can be derived:

$$C = \frac{q \times \delta.\left(\frac{gx}{2}, \frac{gy}{2}, 0\right)}{V} \tag{12}$$

And the photovoltage V is provided as a Boltzmann's relation [10]:

$$V = V_T \times \ln\left(1 + \frac{N_b}{n_i^2} \times \delta\left(\frac{gx}{2}, \frac{gy}{2}, 0\right)\right) \tag{13}$$

For V_T : thermal voltage, k : Boltzmann' constant coefficient, N_b : dosage rate in the cell base and n_i : intrinsic concentration. Combining above results, the capacitance is given as follows:

$$C = \frac{4q^2 \sum_k \sum_j \left(A_{kj} + \sum_i c_i\right) \times \frac{1}{C_k . C_j} \sin\left(C_k \frac{gx}{2}\right) \times \sin\left(C_j \frac{gy}{2}\right)}{k\,T \ln\left(1 + \frac{4}{n_0} \sum_k \sum_j \left(A_{kj} + \sum_i c_i\right) \times \frac{1}{C_k . C_j} \sin\left(C_k \frac{gx}{2}\right) \times \sin\left(C_j \frac{gy}{2}\right)\right)} \tag{14}$$

3. RESULTS AND DISCUSSION

3.1 Excess minority charge carriers in the base

Below in figure 3, carriers' density 3D profile is presented versus both grain size and illumination incidence angles.

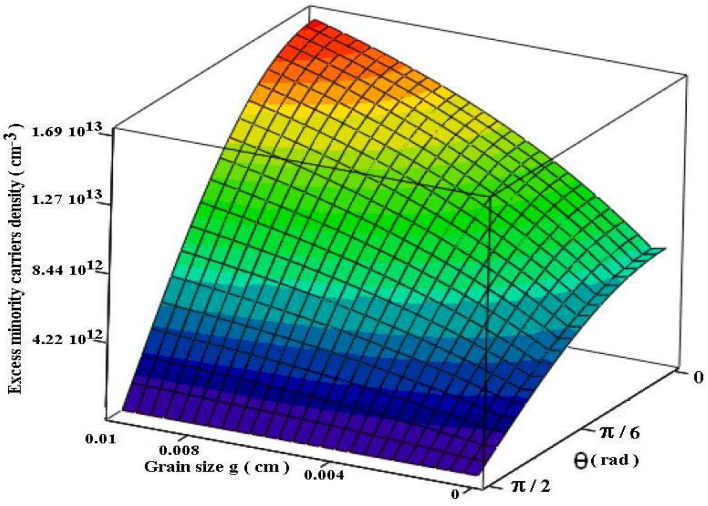

Fig. 3: Carriers density versus both grain size sand illumination angles; Sgb = 10^3 cm/s

As expected, the carriers density increases for an increase in grain size while it decreases when illumination angle increases.

In fact, when the size of any grain decreases, the recombination centres (boundaries' grain) and hence density is affected. Any increase in angle means that normal component (i.e. perpendicular to the junction) of the illumination decreases and negatively affects the generation of carriers in the base.

Below and through the figure 4 we respectively draw the 3D profile of charge carriers density versus both the grain boundary recombination velocity and the angles of incident illumination; while in figure 5, density is also plotted versus velocity (Sgb) but in addition to the grain sizes.

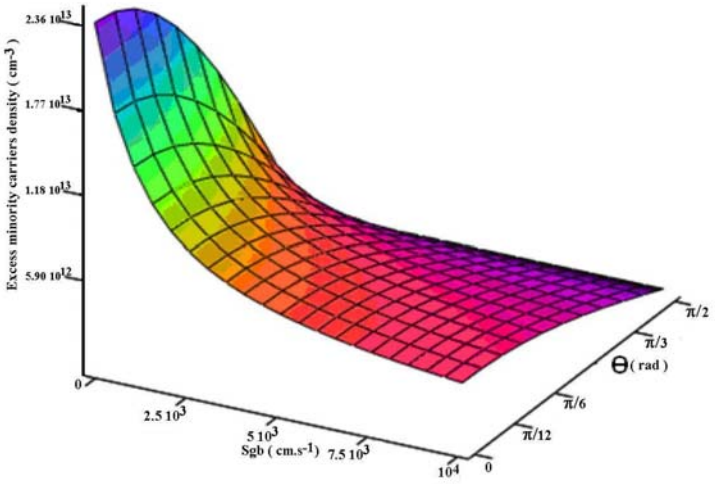

Fig. 4: Charge carriers density versus grain boundary recombination velocity and illumination incidence angles; g = 0.005 cm

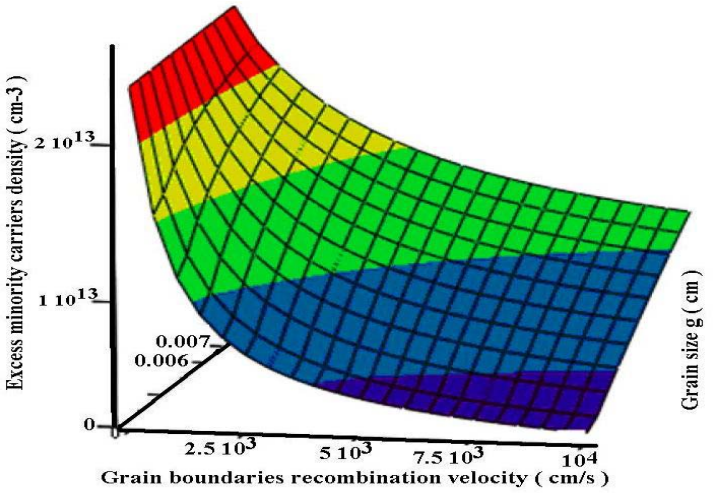

Fig. 5: Charge carriers density versus both the grain sizes and grain boundary recombination velocities; θ = π/4 rad

The results are similar to those found above and it then found that the density is affected by any increase in recombination velocity or in incidence angle; this means that the recombination process become very active once grain boundaries increase in number: then generated electrons can no longer contribute in current flow.

3.2 Capacitance

Through the figure 6, cell capacitance is plotted versus junction recombination velocity for different illumination incidence angles.

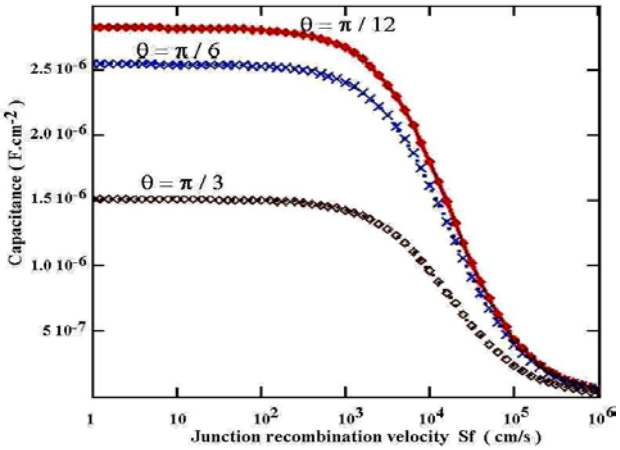

Fig. 6: Capacitance versus junction recombination velocity for different illumination angles; Sgb = 4 10^3 cm/s; g = 0.005 cm

In case of open circuit mode (0 < Sf < 10^3 cm/s) [2, 7], capacitance remains constant for a given angle and this means that generated charge carriers are in fact stored at the junction, a layer separating the emitter from the base.

Instead, capacitance starts to decrease when Sf becomes more important; therefore in short circuit mode (Sf > 10^6 cm/s) [2, 7], there is no more any charge carriers in such above mentioned store- junction: capacitance is becoming more and more poor and photocurrent flow rate very low.

Analysing the influence of incidence angle of illumination on the solar cell, capacitance behaviours poorly once angle is increasing, this in case of open circuit mode.

In fact increasing the illumination incidence angle means that intensity of light is reduced: hence the amount of charge carriers decreases also. But once in short circuit mode, capacitance is very poor and also influence of incidence angle is slow.

Through the below figure 7 profile capacitance profile is plotted versus junction recombination velocity for various sizes of the grain.

Exploiting results from the above figure 7, we find out that capacitance increases with the grain size in case operational points out of the short circuit mode.

Instead, the influence of any variation of the grain size is no longer important while in short circuit mode; in fact capacitance is poor as there are no any carriers stored in the space charge layer.

Over the figure 8, a 3D profile of capacitance is presented versus both the grain sizes and the incidence angles. Findings are similar to those discussed above.

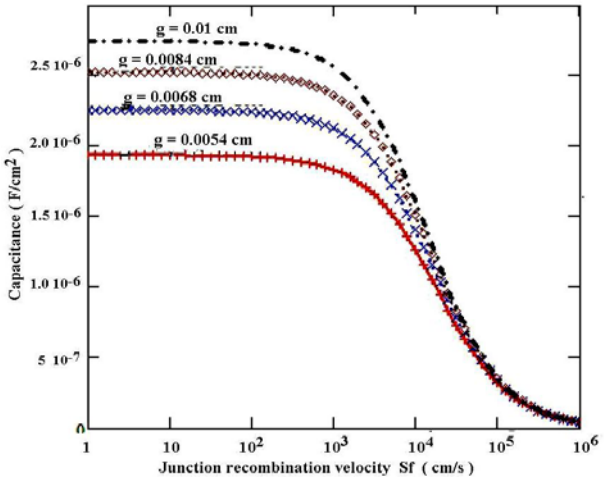

Fig. 7: Capacitance versus junction recombination velocity for different grain sizes; Sgb = 4 10^3 cm/s ; θ = π/4 rad

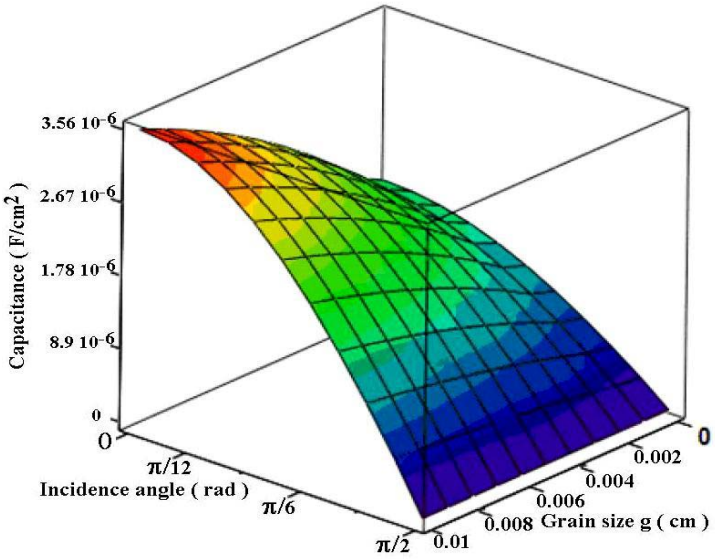

Fig. 8: Capacitance versus grain size and illumination incidence angles; Sgb = 4 10^3 cm/s

Through the below figure 9, the solar cell capacitance is plotted versus the junction recombination velocity, this for different boundary grain recombination velocities (Sgb).

Also it is found that the increase in any recombination velocity affects the capacitance.

Using the figures 10 and 11, a 3D -profile of capacitance is plotted as a quantity influenced by the grain boundary recombination velocity (Sgb), the incidence angles and the grain sizes (g).

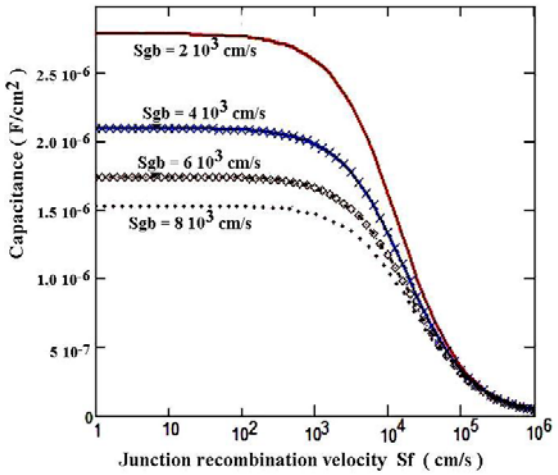

Fig. 9: Capacitance versus junction recombination velocity for different Sgb values; g = 0.005 cm; θ = π/4 rad

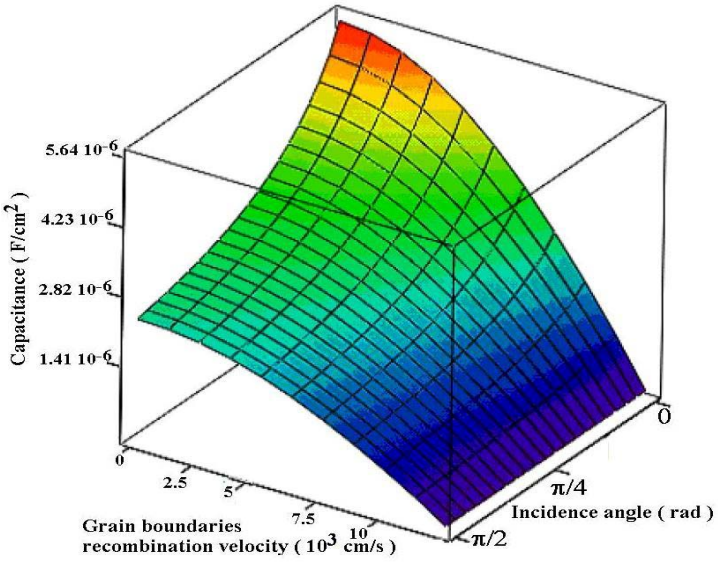

Fig. 10: Capacitance versus Sgb and angles; g = 0.005 cm

3.2.1 Determination of the dark capacitance

Since the diffusion capacitance C and the photovoltage V are both functions of Sf [10], we plotted in figure 12, logarithmic of capacitance versus the photovoltage.

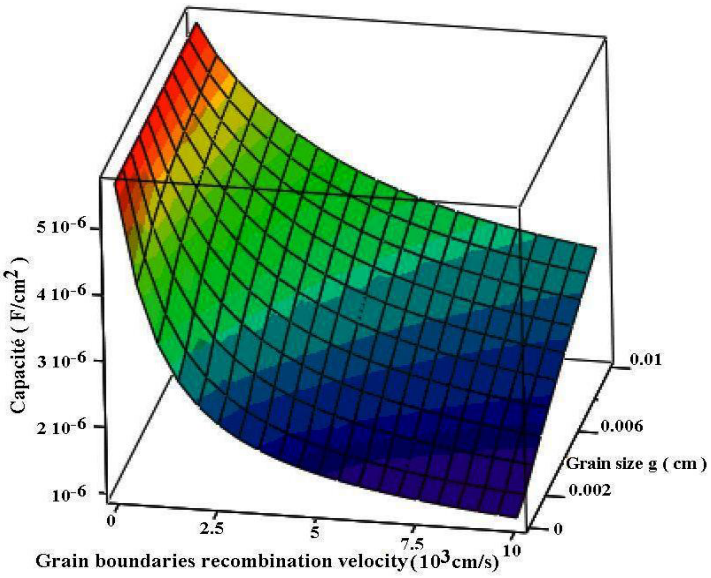

Fig. 11: Capacitance versus Sgb and grain size; θ = π/4 rad

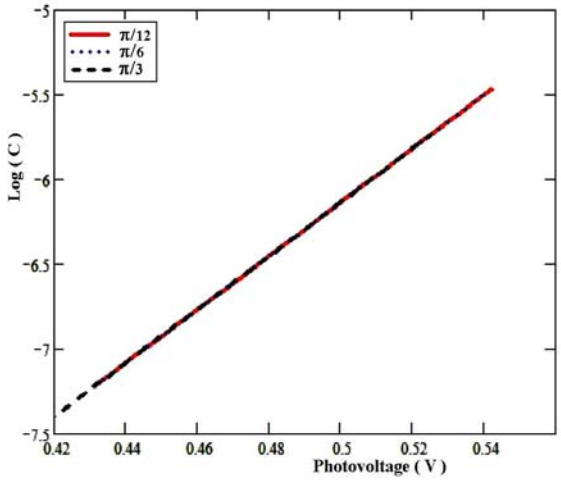

Fig. 12: Logarithmic capacitance versus photovoltage

Extrapoling the graph in figure 12, we obtain the value of the capacitance in case of dark conditions:

$$C_{01} = 410^{-7}\,(F/cm^2) \qquad (15)$$

3.2.2 Capacitance efficiency

As space charges layer in any solar cell behaviours a plate capacitor [10], capacitance is expressed as follows:

$$C = \frac{\varepsilon \,.\, S}{z_o\,(Sf)} \tag{16}$$

Hence, referring to [11], capacitance efficiency is expressed as follows:

$$\eta = 1 - \frac{Z_{oc}}{Z_{cc}} \tag{17}$$

Then the capacitance efficiency becomes:

$$\eta = 1 - \frac{C_{cc}}{C_{co}} \tag{18}$$

Therefore we below plot, through the figure 13, the efficiency of the cell capacitance versus the grain size.

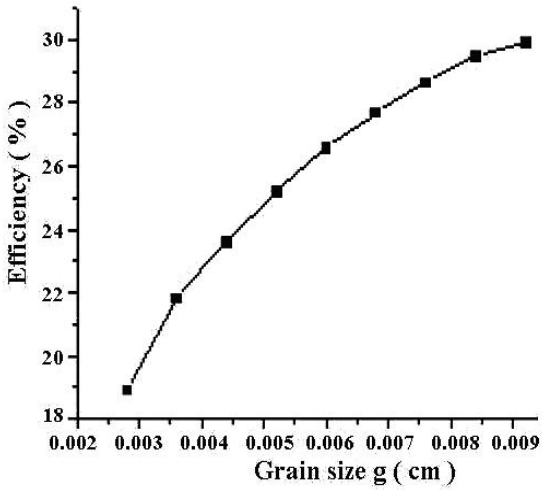

Fig. 13: Capacitance efficiency versus grain size
$\theta = \pi/4$ rad; Sgb = 4 10^3 cm/s

We find out that the efficiency increases with the grain size and reaches its maximum value for a grain size of about 90 µm.

It is also useful to underline that smaller sizes are associated to a numerous multiplication of recombination centres contributing hence in a decrease of the solar cell capacitance efficiency.

In figure 14, we plotted curves of efficiency of the solar cell versus grain boundaries recombination velocity Sgb.

Referring to above figure (Fig. 14), any increase in grain boundary recombination velocity reduces the efficiency of the capacitance; in fact recombination is an action opposite factor to the charge carriers' generation.

Finally, through the below figure (Fig. 15), we highlight the influence of the illumination incidence angles on the solar cell capacitance efficiency.

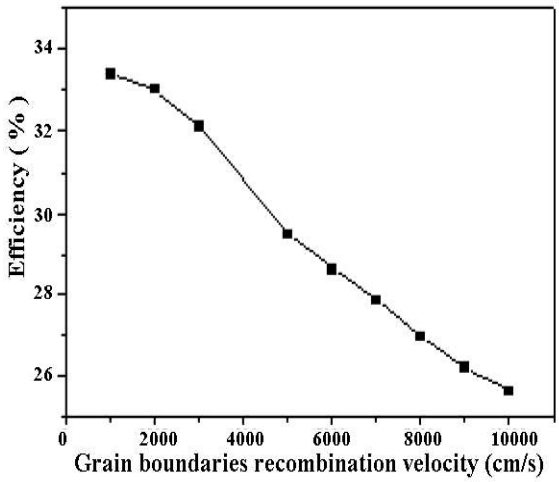

Fig. 14: Capacitance efficiency versus Sgb values
g = 0.01 cm; θ = π/4 rad

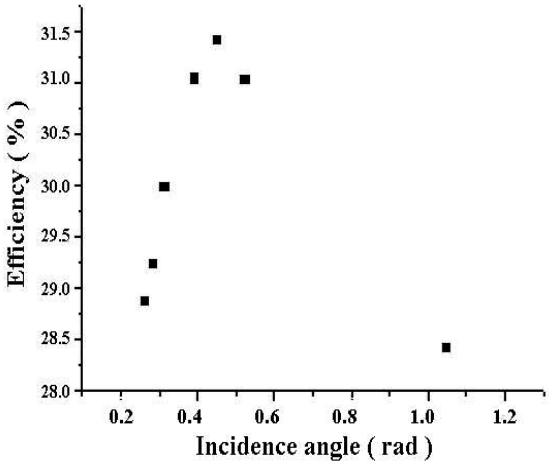

Fig. 15: Capacitance efficiency versus illumination incidence angles
g = 0.01 cm; Sgb = 4 10^3 $cm.s^{-1}$

Even though the capacitance efficiency increases with light incidence angles, a maximum is reached for π/7 rad.

4. CONCLUSION

Through a 3D model study, we analyzed and presented the influence of grain size, grain boundary recombination velocity and illumination incidence angle on a facial solar cell capacitance.

We also calculated the dark capacitance and established and highlighted the behaviour of the solar efficiency. We can conclude that smaller grain sizes are associated to an increasing of recombination centers which act contrarily of charge carriers generation rate.

Two behaviours of efficiency of the solar cell versus the light incidence angles are shown: it increases for $q < \pi/7$ rad and decreases on the other way.

NOMENCLATURE

C : Space charge layer capacitance, ($F.cm^{-2}$)
D: Diffusion coefficient of charge carriers in the solar cell base, ($cm^2.s^{-1}$)
D_{eff}: Effective diffusion coefficient of charge carriers in the cell base, ($cm^2.s^{-1}$)
g : Grain size, (m)
G: Charge carriers' generation ratio, ($N.cm^{-3}.s^{-1}$)
H: Solar cell base thickness, (cm)
L: Minority charge carriers' diffusion length of the solar cell, (cm)
L_{eff}: Effective minority charge carriers' diffusion length of the solar cell, (cm)
q: Elementary electric (positive) charge, (C)
Sb: Back surface minority charge carriers' recombination velocity, ($cm.s^{-1}$)
Sf: Junction minority charge carriers' recombination velocity, ($cm.s^{-1}$)
z: Base depth, (cm)
Sgb: Grain boundary minority charge carriers' recombination velocity, ($cm.s^{-1}$)
Z_{cc}: Base thickness in short circuit mode, cm
Z_{oc}: Base thickness in open circuit mode, (cm)
V_{ph}: Photovoltage, (V)

REFERENCES

[1] H. El Ghitani and S. Martinuzzi, '*Influence of Dislocations on Electrical Properties of Large Grained Polycrystalline Silicon Cells. I: Model*', Journal of Applied Physics, Vol. 66, N°4, pp. 1717 – 1722, 1989.

[2] H.L. Diallo, A. Seïdou Maiga, A. Wereme and G. Sissoko, '*New Approach of Both Junction and Back Surface Recombination Velocities in a 3D Modelling Study of a Polycrystalline Silicon Solar Cell*', The European Physical Journal, Applied Physics, Vol. 42, N°3, pp. 203 – 211, 2008.

[3] S. Mbodji, H. Ly Diallo, I. Ly, A. Dioum, I.F. Barro and G. Sissoko, '*Equivalent Electric Circuit of a Bifacial Solar Cell in Transient State under Magnetic Field*', Proceedings of 21st European Photovoltaic Solar Energy Conference and Exhibition, Dresden, Germany, Poster 1BV.2.49, pp. 457 - 450, 4-8 September, 2006.

[4] J. Dugas, '3*D Modelling of a Reverse Cell Made with Improved Multicrystalline Silicon Wafers*', Solar Energy Materials and Solar Cells, Vol. 32, N°1, pp. 71 – 88, 1994..

[5] J. Furlan and A. Slavko, '*Approximation of the Carrier Generation Rate in Illuminated Silicon*', Solid State Electronics, Vol. 28, N°12, pp.1241 – 1243, 1985

[6] F.I. Barro, S. Mbodji, M. Ndiaye, A.S. Maiga and G. Sissoko, '*Bulk and Surface Recombination Parameters Measurement of Silicon Solar Cell Under Constant White Bias Light*', Journal des Sciences, Vol. 8, N°4, pp. 37 – 41, 2008.

[7] M.L. Samb, M. Dieng, S. Mbodji, B. Mbow, N. Thiam, F.I. Barro and G. Sissiko, '*Recombination Parameters Measurement of Silicon Solar Cell Under Constant White Bias Light*', Proceedings of 24th European Photovoltaic Solar Energy Conference and Exhibition, Hambourg, Germany, Poster 1.CV.4.15., pp. 469 – 472, Sept. 2009.

[8] S. Madougou, F. Made, M.S. Boukary and G. Sissoko, '*I-V Characteristics for Bifacial Silicon Solar Cell Studied Under a Magnetic Field*', Advanced Materials Research, Vol. 18-19. pp. 303 - 312, 2007. Online at *http://www.scientific.net*

[9] G. Sissoko, A. Correa, E. Nanema, M.N. Diarra, A.L. Ndiaye and A. Adj, '*Recombination Parameters Determination in a Double Sided Back-Surface Field Silicon Solar Cell*', Proceeding of the World Renewable Energy Conference and Exhibition, 1856 – 1859, 1998.

[10] G. Sissoko, B. Dieng, A. Correa, M. Adj and D. Azilinin, '*Silicon Solar Cell Space Charge Region Width Determination by Modelling Study*', Proceeding of the World Renewable Energy Conference and Exhibition, 1852 – 1855, 1998.

[11] U.K. Mishra and J. Singh, '*Semiconductor Device Physics and Design*', Edition: Hardcover Publisher: Springer, 2007.